MATHEMATICAL MODELLING OF WATER TREATMENT PROCESSES

SERGEY V. POLYAKOV[1,2], YURI N. KARAMZIN[1], TATIANA A. KUDRYASOVA[1] AND NIKITA I. TARASOV[1]

[1] Keldysh Institute of Applied Mathematics of Russian Academy of Sciences (KIAM RAS)
4 Miusskaya square, 125047 Moscow, Russia

[2] National Research Nuclear University Moscow Engineering Physics Institute (NRNU MEPhi)
31 Kashirskoe shosse, 115409, Moscow, Russia
e-mail: polyakov@imamod.ru, web page: http://www.keldysh.ru

Summary. In this work, the effect of magnetic field on water impurities is studied. The impurities include iron ions and iron oxides. To remove them, magneto-hydrodynamic model is proposed. The problem is considered for the two-dimensional plane-parallel flow. The isothermal laminar flow of fluid is tested. The drift-diffusion approximation is used to show the behavior of the finely dispersed impurities.

1 INTRODUCTION

Water as a natural resource has been a primary concern of man throughout his existence. Total water reserves on Earth are 1386 million cubic kilometers, including water in liquid and frozen forms. But 97.5% of the planet's water resources are saltwater. Freshwater accounts for only 2.5%. Of this fresh water, 99.7% is in the form of ice and permanent snow or in the form of fresh groundwater. Only 0.3% of the fresh water on Earth is in easily accessible. Brazil has more freshwater than any other country.

The growth of the world's population, economic, social and cultural activities of man, the development of industry and new technologies - all these factors negatively affect the environment. The modern producing form of the economy repeatedly "more efficiently" destroys the environment than the historically preceded forms of human life.

Freshwater sustains human life and is vital for human health. In the future, only the world ocean will be the available source to satisfy the human needs with drinking water. To obtain drinking water, clean water for medicine or industrial needs, it is not enough only to desalinate water, it is necessary to purify water from various impurities.

Mathematical modeling of water treatment presents a special challenge because it demands integration of many disciplines. It is dependent on physics, chemistry, mathematics and numerical realization on computer systems to describe the movement of water and the processes of purification. It requires knowledge of the interrelationships of quality water, chemical processes, an understanding of aquatic ecology and medicine. It is important not just to create mathematical models that take into account different physical factors, but to elaborate of technology can be used as a practical tool.

The different aspects of the water treatment by the magnetic field will be proposed in a lot of works (see for example [1-10]). However, there are not much works that connected to the numerical simulation of these processes. This paper concerning with numerical modeling

2010 Mathematics Subject Classification: 65E05, 65Y05, 65Z05, 76U05, 76W05.
Key words and Phrases: Mathematical Modeling, Water Treatment, Magnetic Field.

of water purification by magnetic field in technical systems. For example, we chose the problem of purification of water with iron impurities. Treatment is carried out in a flow tank with non-magnetic walls. For modeling purposes, the hydrodynamic model has been supplemented with the electrostatic equations. The numerical realization is based on standard methods of the theory of finite-difference schemes [11, 12] and on original exponential schemes [13-15]. The implementation of the proposed numerical schemes on spaced grids is performed by iterative methods based on the conjugate gradient scheme [16]. Parallel realization of the numerical procedure based on domain decomposition technique was elaborated in the work [17]. Our previous results on this topic were presented in [18]. In this paper we discuss the results of a more detailed study.

This paper has the following structure. In Section 2, we describe formulation and mathematical description of the problem. In Section 3, we introduce numerical algorithm and parallelization. some details of the numerical algorithm. In Section 4, we propose test calculations. In Section 5 we show results obtained on parallel computer systems, including distribution of stream parameters, distribution of impurity concentration, and distribution of electrical field. In Section 6, we sum up the results and list some topics for future research.

2 PROBLEM FORMULATION AND MATHEMATICAL DESCRIPTION

We discuss the problem of water purification in reservoirs. Real area is shown in Figure 1. Such area can be a part of technical system. It has three holes: one hole is for inlet stream and two holes are for outlet streams.

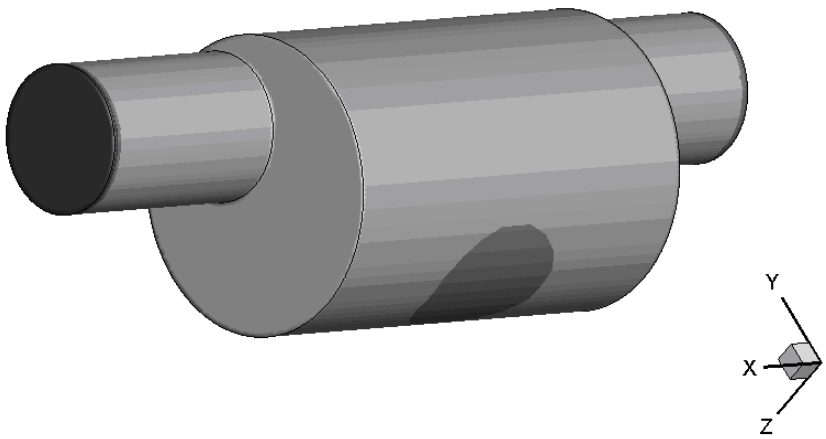

Figure 1. Real 3D domain.

In this work, we study the model problem with real 2D computational domain. It is displayed in Figure 2. Here $L=L_1+L_2+L_3+L_4+L_5$ is length of the area that has size from 5 cm up to 100 cm, $H=H_1+H_2= H_3+H_4$ is height of area that has size from 1 cm up to 10 cm; H_1 is height of the inlet hole, L_3 and H_4 are length and height of the outlet holes. The range of the Reynolds number is 10-100.

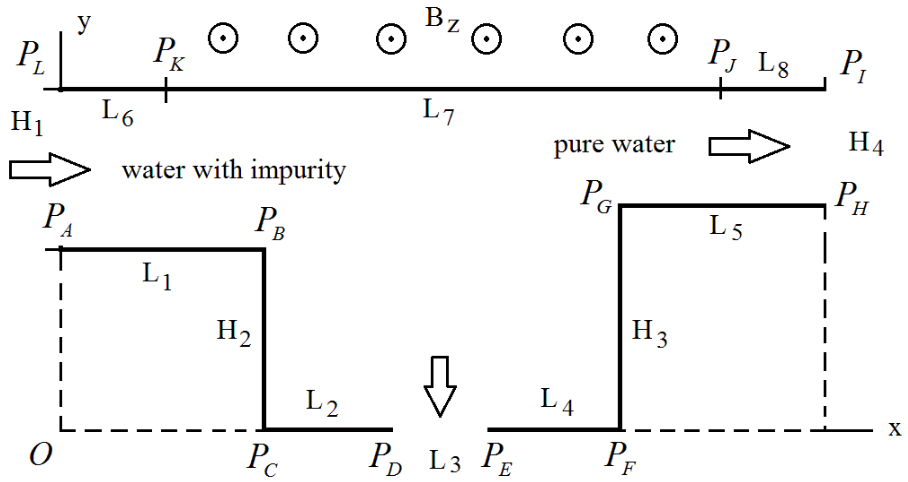

Figure 2. 2D computational area.

The basic equations describe the motion of water with impurities in the incompressible fluid approximation taking into account the presence of an electromagnetic field in the computational domain Ω. It is a section $z=0$ of the original three-dimensional area. It has size $L\times H$ and in the dimensional variables have the form:

$$\frac{\partial \mathbf{u}}{\partial t}+(\mathbf{u}\nabla)\mathbf{u}=-\frac{1}{\rho}\nabla p+\frac{\eta}{\rho}\Delta\mathbf{u}+\mathbf{g},\quad div\,\mathbf{u}=0, \tag{1}$$

$$\frac{\partial C}{\partial t}=div\left(D\nabla C-\mu\mathbf{F}C\right)+(\mathbf{u},\nabla C),\quad \mathbf{F}=\mathbf{E}+[\mathbf{u}\times\mathbf{B}], \tag{2}$$

$$div(\varepsilon\mathbf{E})=q(C-C_0),\quad \mathbf{E}=-\nabla\varphi, \tag{3}$$

Where $\rho=\rho_w+\rho_F=\rho_0\rho(T)$ is the water density with iron ions at the specified temperature T, ρ_w is the water density, ρ_F is the density of iron ions, $\mathbf{u}=(u_x,u_y,0)^T$ is velocity vector of water stream, p is pressure of water stream, $\eta=\eta_0\eta(T)$ and $\nu=\frac{\eta}{\rho}$ are coefficients of dynamic and kinematic viscosity of water stream at the specified temperature, C и C_0 are concentrations of impurity ions and its equilibrium value under conditions of electro neutrality of the flow, $\mathbf{g}=(0,-g,0)^T$ is gravity vector (directed contrarily to the coordinate y), g is gravitational acceleration in the aquatic environment, $D=D_0D(T)$ and $\mu=\mu_0\mu(T)$ are diffusion coefficient and coefficient of ion mobility, q is ion charge in relative units, $\mathbf{F}$ is the total vector field acting on the ions, $\mathbf{E}$ и φ are strength and potential of the electric field, $\mathbf{B}=(0,0,B_0)^T$ is magnetic induction vector, div и ∇ are operators of divergence and gradient in the spatial coordinates (x,y), ε is permittivity of water.

Equations (1)-(3) remain valid and refer to a region Ω, bounded by any closed contour $\partial\Omega$, for example shown on Figure 2. The contour $\partial\Omega$ is defined by a set of control points

$\{P_A, P_B, P_C, P_D, P_E, P_F, P_G, P_H, P_I, P_J, P_K, P_L\}$ and a set of straight line segments that connect these points. It is also understood that the sizes of the computational domain satisfy the relations: $L = L_1 + L_2 + L_3 + L_4 + L_5 = L_6 + L_7 + L_8$, $H = H_1 + H_2 = H_3 + H_4$. The points: P_K and P_J are the boundaries of the action of the magnetic field.

The initial conditions in the case of the real geometry have the form:

$$\begin{aligned} &\mathbf{u} = \mathbf{u}_0(x, y), \quad C = C_0, \quad t = 0, \quad (x, y) \in \Omega; \\ &u_{x,0}(0, y) = u_n(y) = u_0\left[1 - 4\left((y / H_1) - 0.5\right)^2\right], \quad y \in [y_A, y_L]. \end{aligned} \tag{4'}$$

The boundary conditions in the case of the real geometry take the view:

$$\begin{aligned} &u_x = u_n(y), \quad u_y = 0, \quad C = C_0, \quad \frac{\partial \varphi}{\partial x} = 0, \quad (x, y) \in [P_A, P_L]; \\ &\frac{\partial u_x}{\partial x} = 0, \quad \frac{\partial u_y}{\partial x} = 0, \quad \frac{\partial C}{\partial x} = 0, \quad \frac{\partial \varphi}{\partial x} = 0, \quad (x, y) \in [P_H, P_I]; \\ &\frac{\partial u_x}{\partial y} = 0, \quad \frac{\partial u_y}{\partial y} = 0, \quad \frac{\partial C}{\partial y} = 0, \quad \frac{\partial \varphi}{\partial y} = 0, \quad (x, y) \in [P_D, P_E]; \\ &u_x = 0, \quad u_y = 0, \quad \frac{\partial C}{\partial y} = 0, \quad \frac{\partial \varphi}{\partial y} = 0, \quad (x, y) \in [P_A, P_B], [P_C, P_D], [P_E, P_F], [P_G, P_H], [P_I, \\ &u_x = 0, \quad u_y = 0, \quad \frac{\partial C}{\partial x} = 0, \quad \frac{\partial \varphi}{\partial x} = 0, \quad (x, y) \in [P_B, P_C], [P_F, P_G]. \end{aligned} \tag{5'}$$

At moderate velocities, at the entrance to the medium, the flow is rapidly established, and it can be regarded as stationary. To calculate the stationary flow, it is convenient to go from equation (1) to a system of equations in variables ψ (stream function) and ω (vorticity). If we assume that the flow is irrotational and do not take into account gravity, then the water flow can be calculated on the basis of the following Laplace equation:

$$\Delta \psi = \frac{\partial^2 \psi}{\partial x^2} + \frac{\partial^2 \psi}{\partial y^2} = 0, \quad u_x = \frac{\partial \psi}{\partial y}, \quad u_y = -\frac{\partial \psi}{\partial x}, \quad (x, y) \in \Omega \tag{6}$$

The boundary conditions for the stream function in the case of a simple rectangular geometry are as follows:

$$\begin{aligned} &\psi(0, y) = \int_0^y u_n(y)\,dy; \quad \frac{\partial \psi}{\partial x}(L, y) = 0; \\ &\psi(x, 0) = const = \psi_A; \quad \psi(x, H) = const = \psi_B. \end{aligned} \tag{7}$$

Here $\psi_A \neq 0$ is an arbitrary constant and the constant ψ_B satisfies the condition.

$$\psi_B = \psi_A + \int_0^H u_n(y)\,dy \tag{8}$$

In the case of the real geometry, the boundary conditions for the stream function will have the form:

$$\psi(y)=\int_{y_A}^{y} u_n(y)\,dy,\quad (x,y)\in[P_A,P_L];$$
$$\frac{\partial\psi}{\partial x}=0,\quad (x,y)\in[P_H,P_I];\quad \frac{\partial\psi}{\partial y}=0,\quad (x,y)\in[P_D,P_E];$$
$$\psi=const=\psi_A,\quad (x,y)\in[P_A,P_B]\cup[P_B,P_C]\cup[P_C,P_D];\tag{7′}$$
$$\psi=const=\psi_B,\quad (x,y)\in[P_I,P_L];$$
$$\psi=const=\psi_C,\quad (x,y)\in[P_E,P_F]\cup[P_F,P_G]\cup[P_G,P_H].$$

Here the constants: ψ_B and ψ_C satisfy the conditions:

$$\psi_B=\psi_A+\int_{y_A}^{y_L} u_x(0,y)\,dy;\quad \psi_C=\psi_A-\int_{x_D}^{x_E} u_y(x,0)\,dx=\psi_B-\int_{y_H}^{y_I} u_x(L,y)\,dy.\tag{8′}$$

In a more general case, the flow can not be considered as irrotational, and for its description the equations for the stream function and vorticity are used:

$$\frac{\partial^2\psi}{\partial x^2}+\frac{\partial^2\psi}{\partial y^2}=-\omega,\quad \omega=\frac{\partial u_y}{\partial x}-\frac{\partial u_x}{\partial y},\quad u_x=\frac{\partial\psi}{\partial y},\quad u_y=-\frac{\partial\psi}{\partial x},$$
$$\frac{\partial\omega}{\partial t}+div(\mathbf{u}\omega)=\nu\Delta\omega,\quad (x,y)\in\Omega.\tag{9}$$

The vorticity equation will be used in the stationary variant. The boundary conditions for vorticity on solid surfaces are set as follows:

$$\omega=-\frac{\partial u_\tau}{\partial n},\quad (x,y)\in\partial\Omega.\tag{10}$$

Here u_τ is the tangential velocity component, n is the outer normal to the boundary.

It is convenient to represent the equation for concentration in the following equivalent form:

$$\frac{\partial C}{\partial t}=div\,\mathbf{W}+(\mathbf{R},\mathbf{W})+QC,\tag{11}$$

$$\mathbf{W}=D(\nabla C-\mathbf{P}C),\quad \mathbf{P}=q\mu D^{-1}\mathbf{F},\quad \mathbf{R}=D^{-1}\mathbf{u},\quad Q=q\mu D^{-1}(\mathbf{u},\mathbf{F}).\tag{12}$$

In conclusion, we turn to dimensionless variables:

$$x'=x/H,\quad y'=y/H,\quad t'=t/t_0,\quad \Omega'=(0,L)\times(0,1);$$
$$\psi'=\psi/u_0,\quad \omega'=\omega/u_0,\quad \mathbf{u}'=\mathbf{u}/u_0,\quad C'=C/C_0,\quad \varphi'=\varphi/\varphi_0,\quad \mathbf{E}'=\mathbf{E}/E_0;\tag{13}$$
$$t_0=H/u_0,\quad \varphi_0=qn_0H^2/\varepsilon,\quad E_0=\varphi_0/H.$$

Then the final formulation takes the form:

$$\Delta\psi = -\omega, \quad \Delta\omega - div\left(\mathrm{Re}\,\mathbf{u}\omega\right) = 0, \quad u_x = \frac{\partial\psi}{\partial y}, \quad u_y = -\frac{\partial\psi}{\partial x}, \quad (x,y)\in\Omega;$$
$$\frac{\partial C}{\partial t} = \frac{\partial W_x}{\partial x} + R_x W_x + \frac{\partial W_y}{\partial y} + R_y W_y + QC, \tag{14}$$
$$\Delta\varphi = -\left(C-1\right), \quad \mathbf{E} = -\nabla\varphi, \quad (x,y)\in\Omega, \quad t>0;$$

$$\begin{aligned} &\mathbf{W} = D_n D\left(\nabla C - \mathbf{P}C\right), \quad \mathbf{P} = P_n \mu D^{-1}\mathbf{F}, \quad \mathbf{R} = D^{-1}\mathbf{u}, \\ &Q = Q_n \mu D^{-1}\left(\mathbf{u},\mathbf{F}\right), \quad \mathbf{F} = \mathbf{E} + B_n\left[\mathbf{u}\times\mathbf{B}\right], \quad D = D(T), \quad \mu = \mu(T); \\ &\mathrm{Re} = Hu_0/\nu, \quad D_n = D_0/\left(Hu_0\right), \quad P_n = q\mu_0 E_0 u_0^{-1}, \\ &Q_n = q\mu_0 E_0 H D_0^{-1}, \quad B_n = u_0 B_0 E_0^{-1}, \quad E_0 = \varphi_0 H^{-1}. \end{aligned} \tag{15}$$

In the future, we will be neglect the dependences of the diffusion coefficients and mobility on temperature: $D(T)=1$, $\mu(T)=1$. Then the main dimensionless parameters of the problem will be L, D_n, P_n, Q_n, B_n.

Initial conditions take the view:

$$\begin{aligned} &\mathbf{u} = \mathbf{u}_0 = u_n(y)(1,0)^T, \quad C=1, \quad t=0, \quad (x,y)\in\Omega; \\ &u_n(y) = 1-4(y-0.5)^2. \end{aligned} \tag{16}$$

Boundary conditions takes the view:

$$\begin{aligned} &x=0: \quad \psi = \int_0^y u_n(y)\,dy, \quad \omega=0, \quad u_x = u_n(y), \quad u_y=0, \quad C=1, \quad \frac{\partial\varphi}{\partial x}=0; \\ &x=L: \quad \frac{\partial\psi}{\partial x}=0, \quad \frac{\partial\omega}{\partial x}=0, \quad \frac{\partial u_x}{\partial x}=0, \quad \frac{\partial u_y}{\partial x}=0, \quad \frac{\partial C}{\partial x}=0, \quad \frac{\partial\varphi}{\partial x}=0; \\ &y=0,1: \quad \frac{\partial\psi}{\partial x}=0, \quad \omega = -\frac{\partial^2\psi}{\partial x^2}, \quad \frac{\partial u_x}{\partial y}=0, \quad u_y=0, \quad \frac{\partial C}{\partial y}=0, \quad \frac{\partial\varphi}{\partial y}=0. \end{aligned} \tag{17}$$

3 NUMERICAL ALGORITHM AND PARALLELIZATION

To solve the problem, it is proposed to use the finite difference method. For this, we introduce in the domain Ω a uniform space grids $\Omega_h = \omega_x\times\omega_y$, $\overline{\Omega}_h = \overline{\omega}_x\times\overline{\omega}_y$ and grid on time $\omega_t = \left\{t_k = \tau\cdot k, k=0,\ldots,N_t\right\}$. The space grids are multiplication of the following one-dimensional grids:

$$\begin{aligned} &\omega_x = \left\{x_i = h_x\cdot i, i=0,\ldots,N_x, h_x = L/N_x\right\}, | \, \omega_y = \left\{y_j = h_y\cdot j, j=0,\ldots,N_y, h_y = 1/N_y\right\}, \\ &\overline{\omega}_x = \left\{x_{i-1/2} = 0.5\left(x_{i-1}+x_i\right), i=1,\ldots,N_x\right\}, \ \overline{\omega}_y = \left\{y_{j-1/2} = 0.5\left(y_{j-1}+y_j\right), j=1,\ldots,N_y\right\}. \end{aligned} \tag{18}$$

Here N_x, N_y are numbers of grid segments on x and y, τ is step on time, N_t is number of steps. For setting of real geometry we use the markers of cells.

The stream function is defined on the grid Ω_h (i.e. nodes), and the rest functions are defined on the grid $\bar{\Omega}_h$ (i.e., in the cell centers). For the stream function, the velocity vector, and the potential of the electric field, we write the following standard difference equations [11, 12], supplementing them, if necessary, with the boundary conditions:

$$\begin{aligned} &\Lambda_h \psi_h \equiv (\psi_h)_{x\bar{x}} + (\psi_h)_{y\bar{y}} = -\omega_h, \quad (x,y) \in \Omega_h; \\ &u_{x,h} = 0.5(\psi_{h,y} + \psi_{h,\bar{y}}), \quad u_{y,h} = -0.5(\psi_{h,x} + \psi_{h,\bar{x}}), \quad (x,y) \in \bar{\Omega}_h; \\ &\Lambda_h \varphi_h \equiv (\varphi_h)_{x\bar{x}} + (\varphi_h)_{y\bar{y}} = -(C_h - 1), \quad (x,y) \in \bar{\Omega}_h. \end{aligned} \tag{19}$$

To approximate the equation for a vortex, we write it in the form by applying a single integral transformation:

$$\begin{aligned} &\frac{\partial}{\partial x}\left(W_x^{(\omega)}\right) + \frac{\partial}{\partial y}\left(W_y^{(\omega)}\right) = 0, \\ &W_x^{(\omega)} = \frac{1}{e_x^{(\omega)}} \frac{\partial}{\partial x}\left(e_x^{(\omega)} \frac{\partial \omega}{\partial x}\right), \quad W_y^{(\omega)} = \frac{1}{e_y^{(\omega)}} \frac{\partial}{\partial y}\left(e_y^{(\omega)} \frac{\partial \omega}{\partial y}\right), \\ &e_x^{(\omega)} = \exp\left[-\int_0^x \mathrm{Re}\, u_x dx'\right], \quad e_y^{(\omega)} = \exp\left[-\int_0^y \mathrm{Re}\, u_y dy'\right]. \end{aligned} \tag{20}$$

Then the exponential scheme for the given equation in accordance with [13-15] is as follows:

$$\Lambda_h^{(\omega)} \omega_h \equiv \Lambda_{h,x}^{(\omega)} \omega_h + \Lambda_{h,y}^{(\omega)} \omega_h = 0, \tag{21}$$

$$\begin{aligned} &\Lambda_{h,x}^{(\omega)} \omega_h = \frac{1}{\hbar_x} \left\{ \frac{\tilde{e}_x^{(\omega)}(x+h_x)\,\omega_h(x+h_x) - \omega_h(x)}{0.5\left(\tilde{e}_x^{(\omega)}(x+h_x)+1\right)h_x} - \frac{\tilde{e}_x^{(\omega)}(x)\,\omega_h(x) - \omega_h(x-h_x)}{0.5\left(\tilde{e}_x^{(\omega)}(x)+1\right)h_x} \right\}, \\ &\Lambda_{h,y}^{(\omega)} \omega_h = \frac{1}{\hbar_y} \left\{ \frac{\tilde{e}_y^{(\omega)}(y+h_y)\,\omega_h(y+h_y) - \omega_h(y)}{0.5\left(\tilde{e}_y^{(\omega)}(y+h_y)+1\right)h_y} - \frac{\tilde{e}_y^{(\omega)}(y)\,\omega_h(y) - \omega_h(y-h_y)}{0.5\left(\tilde{e}_y^{(\omega)}(y)+1\right)h_y} \right\}, \end{aligned} \tag{22}$$

$$\begin{aligned} &\tilde{e}_x^{(\omega)}(x+h_x) = \frac{e_x^{(\omega)}(x+h_x)}{e_x^{(\omega)}(x)} = \exp\left[-\int_x^{x+h_x} \mathrm{Re}\, u_x dx'\right] \approx \exp\left[-\mathrm{Re}\, h_x u_x (x+0.5h_x)\right], \\ &\tilde{e}_x^{(\omega)}(x) = \frac{e_x^{(\omega)}(x)}{e_x^{(\omega)}(x-h_x)} = \exp\left[-\int_{x-h_x}^{x} \mathrm{Re}\, u_x dx'\right] \approx \exp\left[-\mathrm{Re}\, h_x u_x (x-0.5h_x)\right], \end{aligned} \tag{23}$$

$$\tilde{e}_y^{(\omega)}\left(y+h_y\right)=\frac{e_y^{(\omega)}\left(y+h_y\right)}{e_y^{(\omega)}\left(y\right)}=\exp\left[-\int\limits_{y}^{y+h_y}\mathrm{Re}\,u_y dy'\right]\approx\exp\left[-\mathrm{Re}\,h_y u_y\left(y+0.5h_y\right)\right],$$
$$\tilde{e}_y^{(\omega)}\left(y\right)=\frac{e_y^{(\omega)}\left(y\right)}{e_y^{(\omega)}\left(y-h_y\right)}=\exp\left[-\int\limits_{y-h_y}^{y}\mathrm{Re}\,u_y dy'\right]\approx\exp\left[-\mathrm{Re}\,h_y u_y\left(y-0.5h_y\right)\right]. \quad (23')$$

To approximate the equation for the concentration, we write it in the transformed form, applying the double integral transformation [13-15]:

$$\frac{\partial C}{\partial t}=\frac{1}{g_x}\frac{\partial}{\partial x}\left(g_x W_x\right)+\frac{1}{g_y}\frac{\partial}{\partial y}\left(g_y W_y\right)+QC, \quad (24)$$

$$g_x=\exp\left[\int\limits_0^x R_x dx'\right],\quad g_y=\exp\left[\int\limits_0^y R_y dy'\right],\quad R_x=u_x,\quad R_y=u_y,$$
$$W_x=D_n\left(\frac{\partial C}{\partial x}-P_x C\right)=D_n\frac{1}{e_x}\frac{\partial}{\partial x}\left(e_x C\right),\quad W_y=D_n\left(\frac{\partial C}{\partial y}-P_y C\right)=D_n\frac{1}{e_y}\frac{\partial}{\partial y}\left(e_y C\right),$$
$$e_x=\exp\left[-\int\limits_0^x P_x dx'\right],\quad e_y=\exp\left[-\int\limits_0^y P_y dy'\right],\quad Q=Q_n\left(u_x F_x+u_y F_y\right),$$
$$P_x=P_n F_x,\quad P_y=P_n F_y,\quad F_x=E_x+B_n u_y,\quad F_y=E_y-B_n u_x. \quad (25)$$

For it we write the following explicitly - implicit difference scheme, supplemented by the corresponding boundary conditions:

$$\frac{\hat{C}_h-C_h}{\tau}=\bar{\Lambda}_h\hat{C}_h+Q_h\hat{C}_h,\quad C_h\big|_{t=0}=1, \quad (26)$$

Here operator $\bar{\Lambda}_h$ is defined as follows:

$$W_{x,h}=D_n\frac{1}{e_{x,h}}\left(e_{x,h}C_h\right)_x,\quad W_{y,h}=D_n\frac{1}{e_{y,h}}\left(e_{y,h}C_h\right)_y,$$
$$e_{x,h}=\exp\left[-\sum_{0\le x'\le x}P_{x,h}h_x\right],\quad e_{y,h}=\exp\left[-\sum_{0\le y'\le y}P_{y,h}h_y\right]. \quad (27)$$

The realization of the constructed schemes is performed using iterative algorithms based on conjugate gradients scheme [16]. Parallel implementation of the algorithm is based on the domain decomposition technique elaborated in [17] and shown on Fig. 3. Also we used parallel versions of iterative procedures [16]. Computer implementation is performed using MPI and OpenMP technologies.

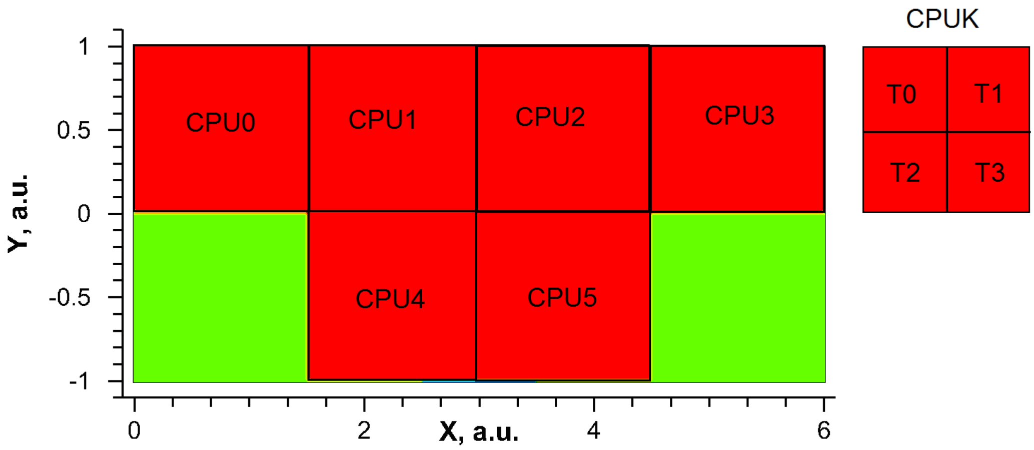

Figure 3. Domain decomposition technique for distribution of calculations on CPUs and threads of CPU.

4 TESTING OF NUMERICAL METHOD

The testing of the proposed numerical procedure was carried out for the case of simplified rectangular geometry (see Fig. 4). For testing, the calculation option was chosen without taking into account the vorticity of the water flow ($\omega = 0$). In tests the following parameters were used: $L = 6$, $D_n = 1$, $P_n = 1$, $Q_n = 1$, $B_n = 1$. Grid parameters were: $N_x = 300$, $N_y = 50$, $h_x = h_y = 0.02$, $\tau = 10^{-4}$.

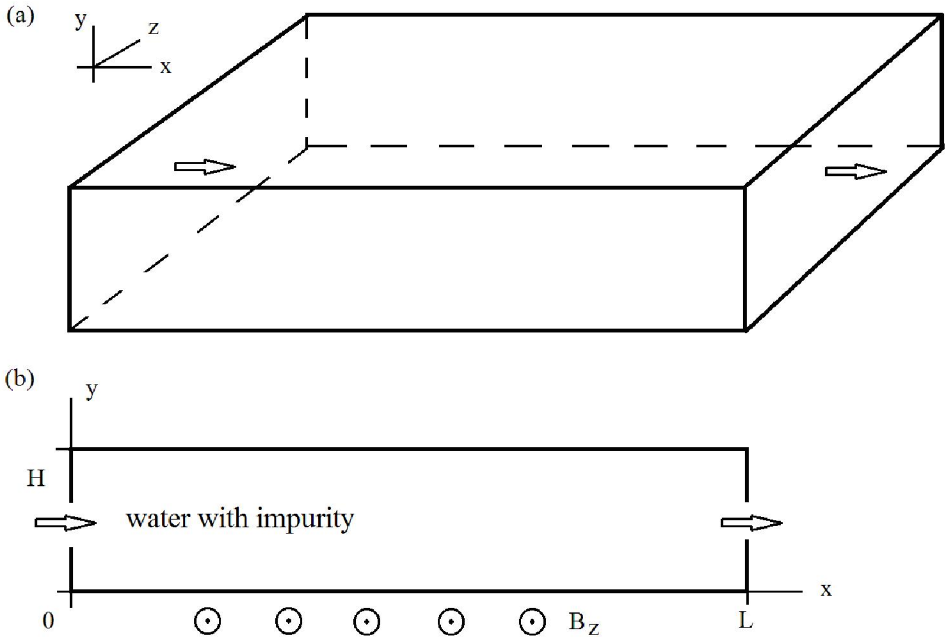

Figure 4. Plane computational area.

The results of the calculations are shown in Fig. 5-8. They are respectively represented by distributions of the current function, the velocity modulus, and also the stationary distributions of the electric field potential and the impurity concentration. The analysis of the obtained data shows the following. In the case of positive values of B_n, parameter of the magnetic field influence leads to decrease of the ion concentration in the upper part of the region and the formation of increased concentration of ions in the lower layer. Thus, the general expected physical effect is realized, namely, cleaning of the upper layer of water from the impurity.

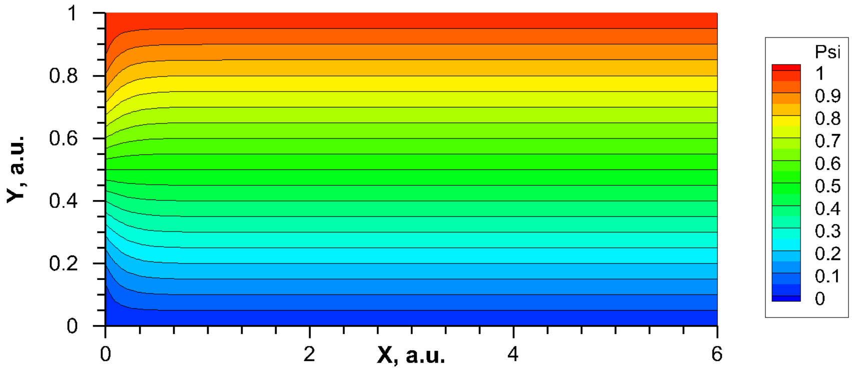

Figure 5. Distribution of flow function.

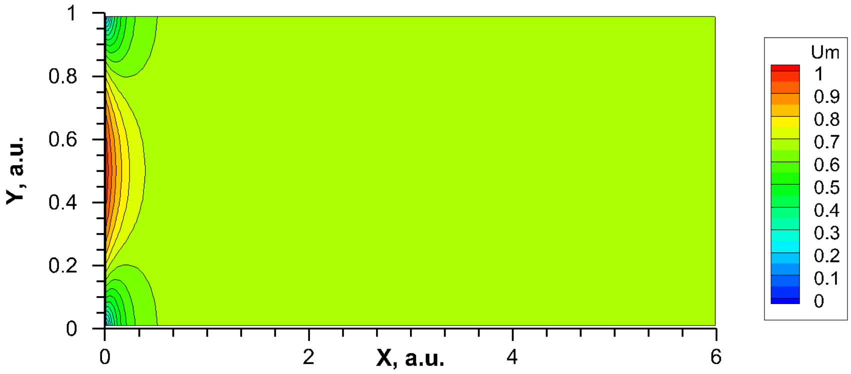

Figure 6. Distribution of velocity modulus.

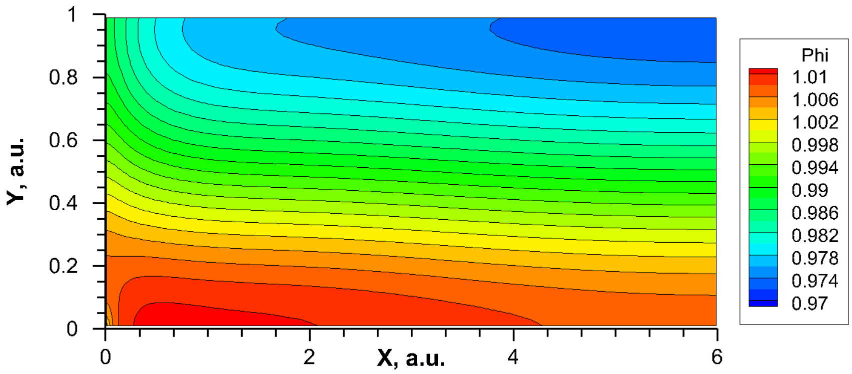

Figure 7. Steady state distribution of electrical field potential.

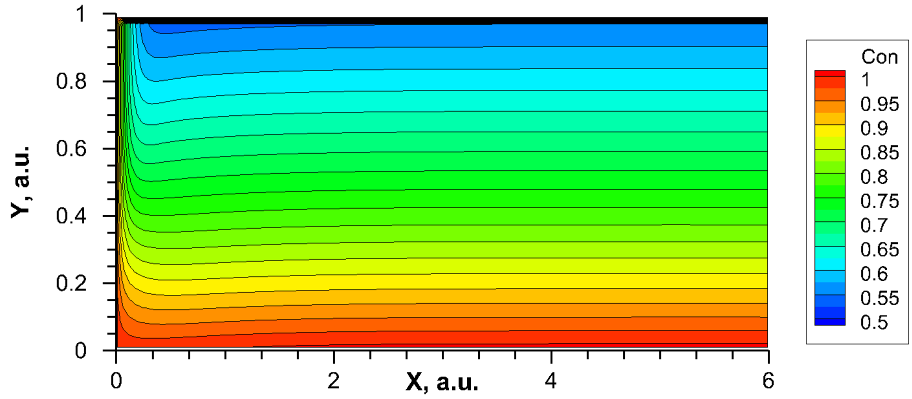

Figure 8. Steady state distribution of impurity concentration.

The degree of cleaning depends on the parameter B_n. Purification becomes noticeable, when the Lorentz force is comparable to the hydrodynamic pressure, that is $B_n \sim 1$. The performed calculations show that the decrease of the impurity concentration in the upper layer of the liquid reaches approximately 2 times for $B_n = 1$. If $B_n = 2$, then the decreasing of the impurity concentration achieves to 3.5 times (see Fig. 9).

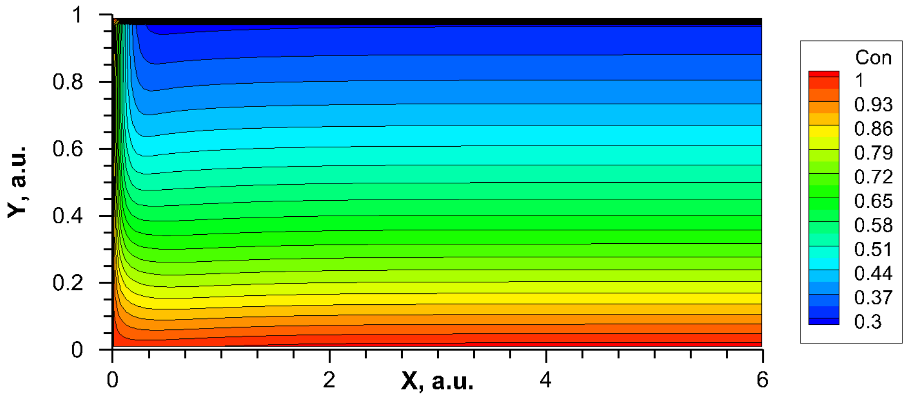

Figure 9. Steady state distribution of impurity concentration for $B_n = 2$.

The spatially localized effect of the magnetic field is realized in industrial cleaning systems. In this paper, we have introduced the dependence on the parameter B_n on the longitudinal coordinate x. For an example, we considered the localization of a magnetic field in the region $x \in [1.5, 4.5]$ and $B_n = 1$. The results of the calculations are presented in Fig. 10, 11. They show that the layer of purified water is located in the upper part of the localized area, that is, also localized.

Calculations on the sequence of grids have shown that the obtained distributions of all unknown functions are reproduced with an error proportional to the error in the approximation of the finite-difference schemes $\Psi = O\left(h_x^2 + h_y^2\right)$. Thus, the presented numerical procedure is correct.

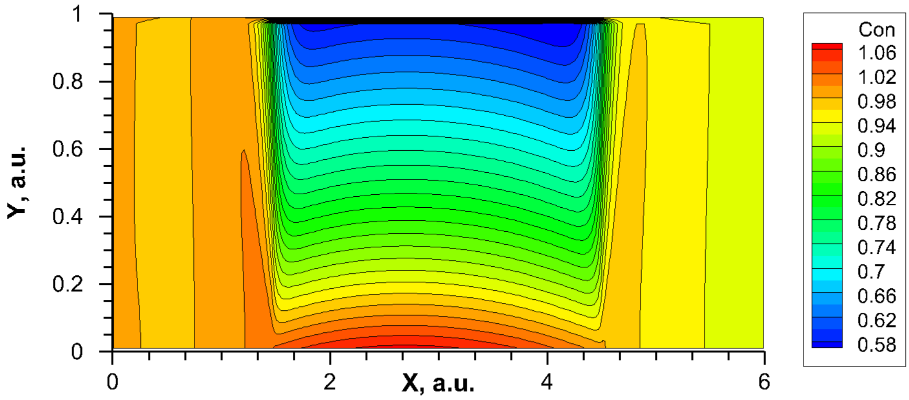

Figure 10. Steady state distribution of impurity concentration for case of localized magnetic field with amplitude $B_n = 1$.

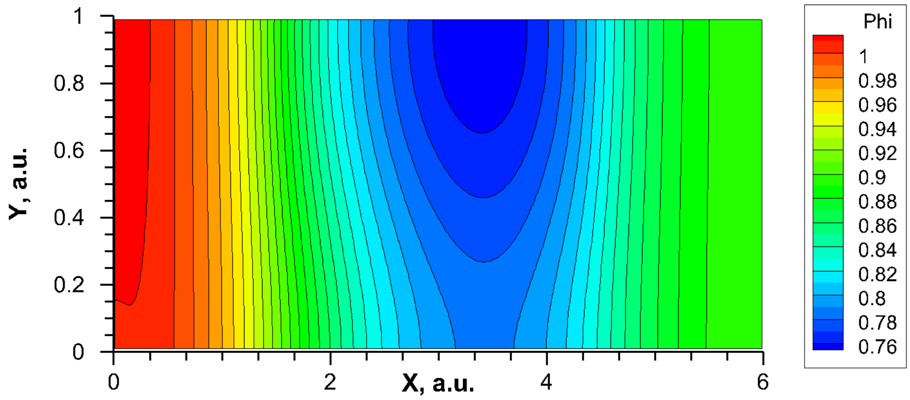

Figure 11. Steady state distribution of electric field potential for case of localized magnetic field with amplitude $B_n = 1$.

5 REAL GEOMETRY CASE

In the case of a real two-dimensional geometry, calculations were performed on grids with parameters $N_x = 600$, $N_y = 100$, $h_x = h_y = 0.01$, $\tau = 5 \cdot 10^{-5}$. The results of calculations are considered for case of the symmetric computational domain with parameters $L = 6$, $L_1 = L_5 = 1.5$, $L_2 = L_3 = L_4 = 1.0$, $H = 2$, $H_1 = H_2 = H_3 = H_4 = 1$ (see Fig. 12). Other task parameters were equal $D_n = 1$, $P_n = 1$, $Q_n = 1$, $B_n = 3$. The magnetic field was localized in the area of the discharge hopper ($L_6 = L_8 = 1.5$, $L_7 = 3$). The calculations were carried out both in the irrotational approximation ($\omega = 0$) and with vorticity for the Reynolds number $\mathrm{Re} = 10$.

Calculations without the vorticity and with it are presented in Fig. 13-16. They show that the vorticity consideration gives a more accurate physical picture. With this geometric configuration, the impurity is concentrated in the lower left corner of the discharge hopper . The cleaning effect is localized in the upper part of the discharge hopper.

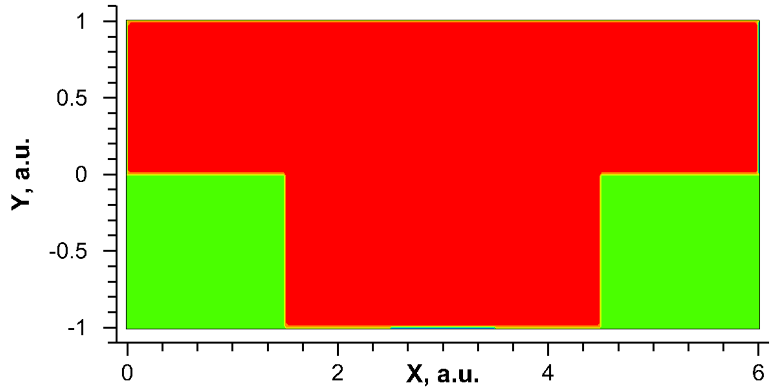

Figure 12. Distribution of markers defining of real geometry.

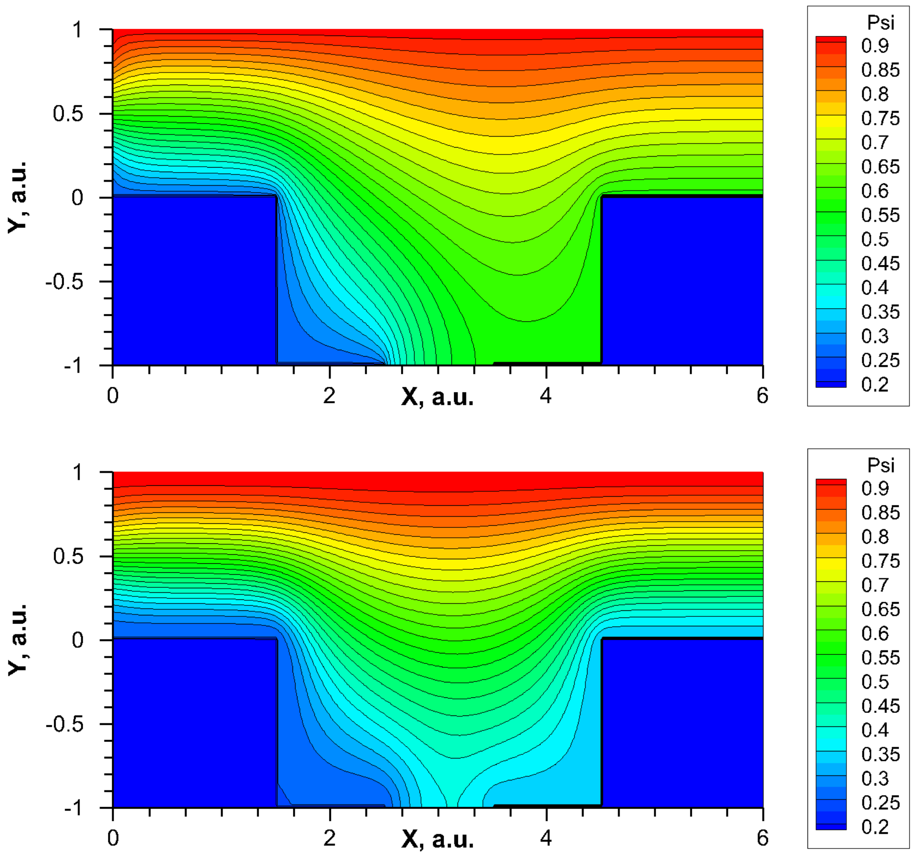

Figure 13. Distribution of flow function for two cases:
$\omega \equiv 0$ (top figure) and $\omega \neq 0$ (bottom figure).

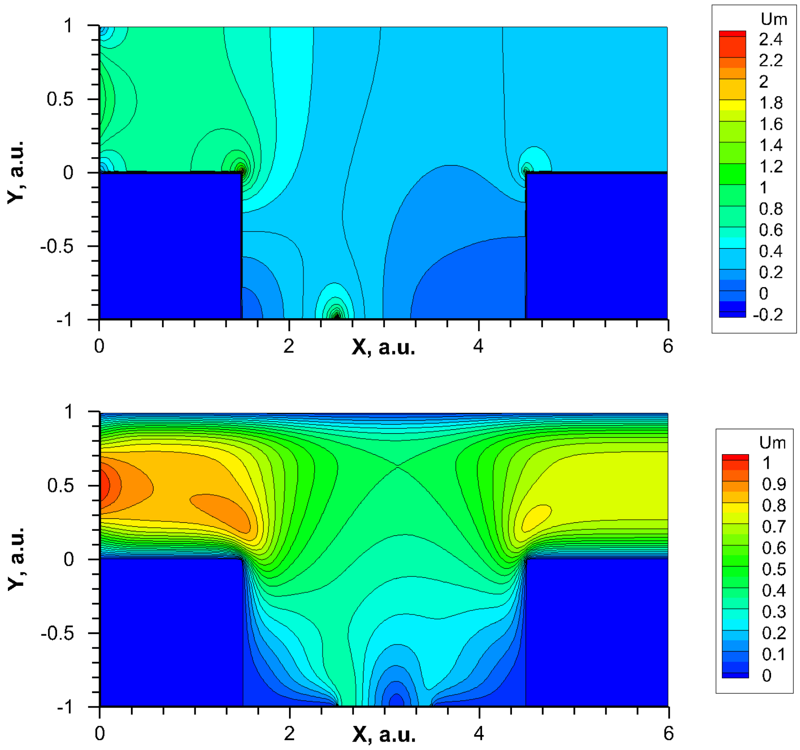

Figure 14. Distributions of velocity modulus for two cases:
$\omega \equiv 0$ (top figure) and $\omega \neq 0$ (bottom figure).

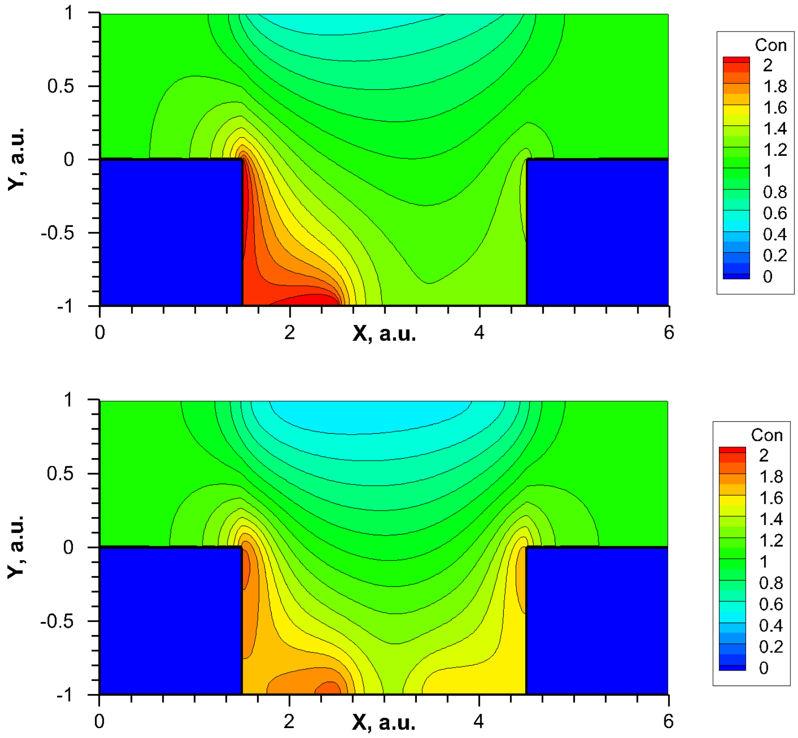

Figure 15. Steady state distributions of impurity concentration for two cases:
$\omega \equiv 0$ (top figure) and $\omega \neq 0$ (bottom figure).

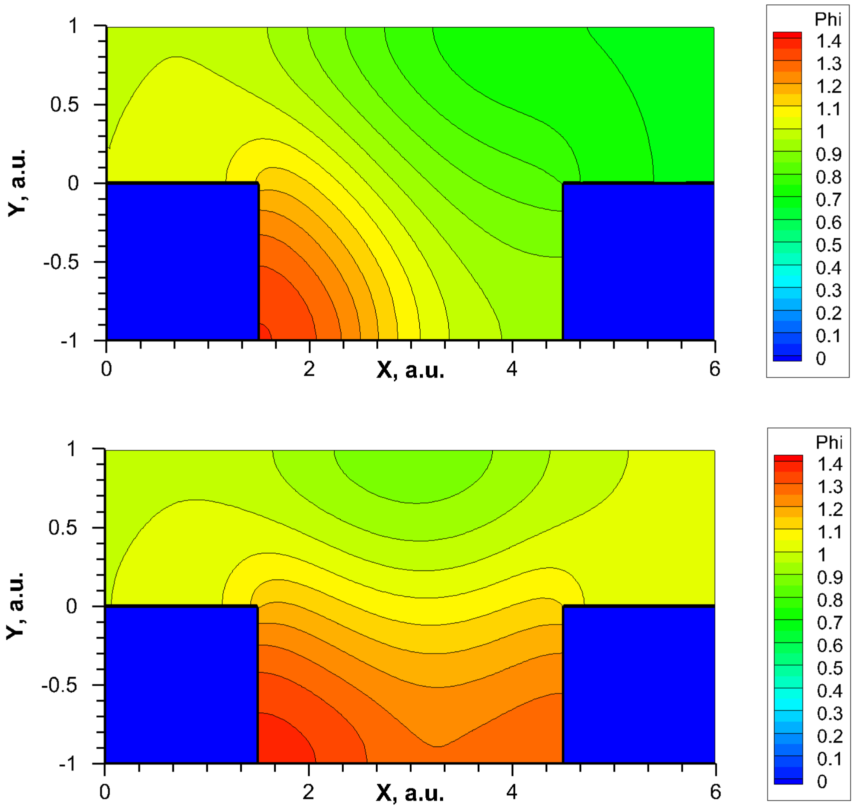

Figure 16. Steady state distributions of electrical field potential for two cases: $\omega \equiv 0$ (top figure) and $\omega \neq 0$ (bottom figure).

Also, calculations were made for the case of an asymmetric design of a magnetic purification system (Fig. 17). The outlet channel was 2 times as wide as the inlet channel, and the drainage hole from the hopper was shifted to the right: $L_1 = L_5 = 1.5$, $L_2 = 1.9$, $L_3 = 1.0$, $L_4 = 0.1$, $H_1 = H_2 = 1$, $H_3 = 1.5$, $H_4 = 0.5$. The results of the calculations are presented in Fig. 18-20. They show that with this design of the magnetic purification system, the purified water is discharged through the right output with a purification degree of about 50%. Thus, the cleaning control can be performed both by increasing the magnetic field value and by optimizing the geometric parameters.

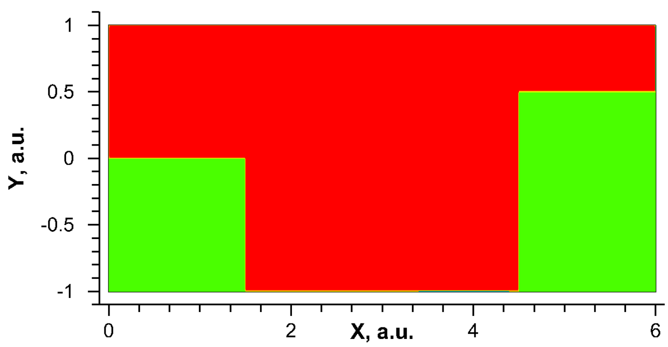

Figure 17. Distribution of markers that determines the real non-symmetrical geometry.

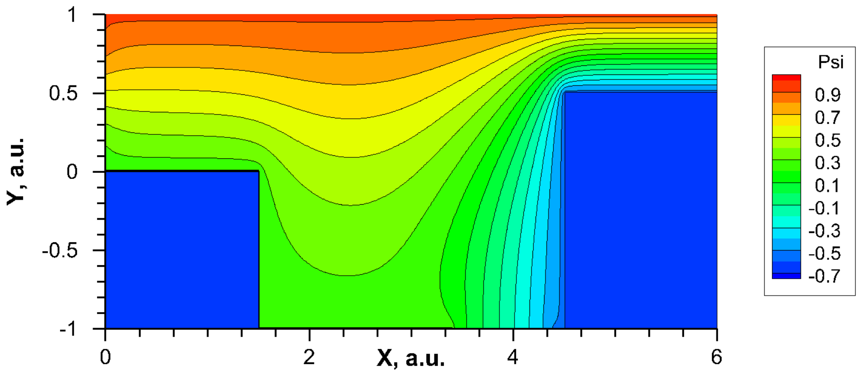

Figure 18. Distribution of flow function.

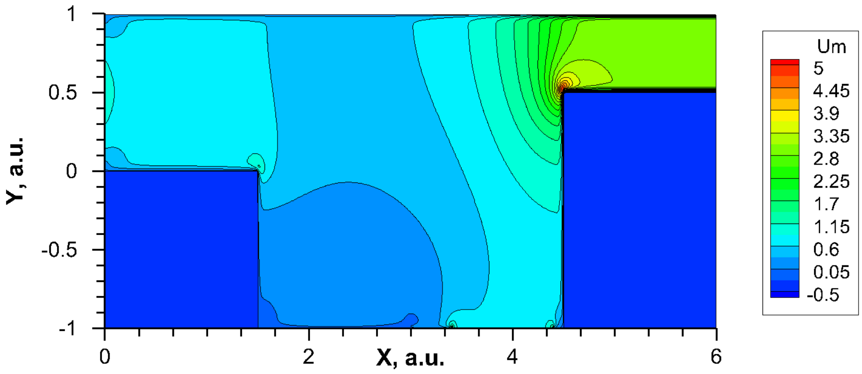

Figure 19. Distribution of velocity modulus.

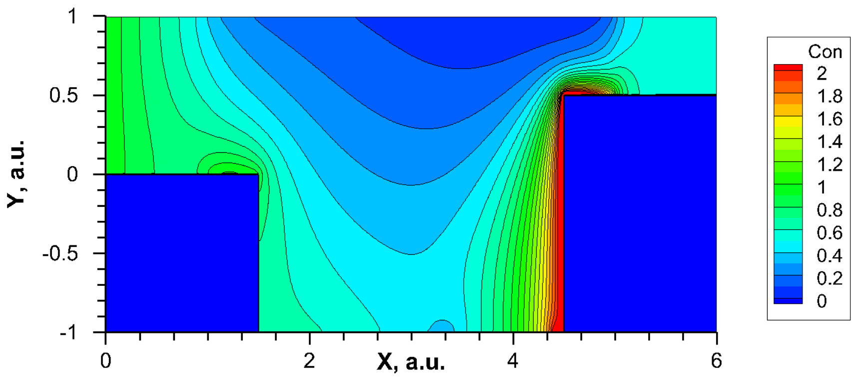

Figure 20. Steady state distribution of impurity concentration.

6 CONCLUSIONS

In the work the actual problem of water purification from iron impurities with the help of electro-magnetic methods is considered. For the model problem, the numerical method and parallel algorithm for computer experiments are proposed. Testing the program on parameter sets confirmed the operability of the proposed computational approach. With the help of the developed technique, some details of the cleaning process were considered. In the future it is proposed to analyze the full three-dimensional model and take into account the chemical transformations.

Acknowledgements: This work was performed as part of the Soyuz SKIF-Nedra Science and Engineering Program with the financial support of the Ministry of Education and Science of the Russian Federation (GK No. 14.964.11.0001 dated June 17, 2015).

REFERENCES

[1] V.I. Shvets, A.M. Yurkevich, O.V. Mosin, and D. A Skladnev, “Preparation of deuterated inosine suitable for biomedical application”, *Journal of Medical Sciences*, **8**(4), 231-232 (1995).
[2] M.R. Powell, “Magnetic Water and Fuel Treatment: Myth, Magic, or Mainstream Science?” *Skeptical Inquirer*, **22** (1) (1998) URL: https://www.csicop.org/SI/archive/category/volume_22.1
[3] J.M.D. Coey, S. Cass, “Magnetic water treatment”, *Journal of Magnetism and Magnetic Materials*, **209**, 71-74 (2000).
[4] A. Szkatula, M. Balanda, M. Kopec, “Magnetic treatment of industrial water. Silica activation”, *The European Physical Journal Applied Physics*, **18**, 41-49 (2002).
[5] V.F. Ochkov, and J. Chudova, “Magnetic water treatment: history and the current state”, *Energy saving and water treatmen,* **1**, 122-134 (2013).
[6] F. Alimi, M.M. Tlili, M.B. Amor, G. Maurin, C. Gabrielli, “Effect of magnetic water treatment on calcium carbonate precipitation: Influence of the pipe material”, *Chemical Engineering and Processing: Process Intensification*, **48** (8), 1327(1-18 (2009).
[7] Z. Jia et al. “Preparation and Application of Novel Magnetically Separable r-Fe2O3/Activated Carbon Sphere Adsorbent”, *Material Science and Engineering*, *B,* **176**, 861-865 (2011).
[8] S. Chaturvedi, P.N. Dave, “Removal of iron for safe drinking water”, *Desalination,* **303**, 1-11 (2012).
[9] M. Lu et al. “Surface modification of porous suspended ceramsite used for water treatment by activated carbon/Fe3O4 magnetic composites”, *Environmental Technology,* **34**, 2301-2307 (2013).
[10] S.I. Koshoridze, Yu.K. Levin, "Magnetic Ultrasonic Water Treatment", *Physical-Chemical Kinetics in Gas Dynamics*, **4**, 534(1-8) (2015).
[11] A.A. Samarskii, *The Theory Of Difference Schemes*, New York: Marcel Dekker, Inc., (2001).
[12] A.A. Samarskii and P.N. Vabishchevich, *Numerical methods for solving inverse problems of mathematical physics*, Walter de Gruyter, (2007).
[13] S.V. Polyakov, “Exponential difference schemes for convection-diffusion equation”, *Mathematica Montisnigri*, **XXV**, 1-16 (2012).
[14] S.V. Polyakov, “Exponential Difference Schemes with Double Integral Transformation for Solving Convection-Diffusion Equations”, *Mathematical Models and Computer Simulations*, **5(4)**, 338-340 (2013).
[15] S.V. Polyakov, Yu.N. Karamzin, T.A. Kudryashova, I.V. Tsybulin, “Exponential Difference Schemes for Solving Boundary-Value Problems for Diffusion-Convection-type Equations”, *Mathematical Models and Computer Simulations*, **9**(1), 71-82 (2017).
[16] A.A. Samarskii and E.S. Nikolaev, *Numerical Methods for Grid Equations*, Vol. I: Direct Methods, Vol. II: Iterative Methods, Basel-Boston-Berlin, Birkhäuser Verlag, (1989).
[17] I.A. Graur, T.G. Elizarova, T.A. Kudryashova, and S.V. Polyakov, “Numerical investigation of jet flows, using multiprocessor computer systems”, *Mathematical Modelling*, **14**(6), 51-62 (2002).
[18] T. Kudryashova, S. Polyakov, “Mathematical modeling of water purification process of iron containing impurities”, *Proceedings of the Tenth International Conference on Advanced Engineering Computing and Applications in Sciences, IARIA XPS Press, Wilmington*, USA, 29-34 (2016).

Received October 1, 2017